

# The C IV Baldwin effect in QSOs from Seventh Data Release of the Sloan Digital Sky Survey

Wei-Hao Bian<sup>1</sup>, Li-Ling Fang<sup>1</sup>, Ke-Liang Huang<sup>1</sup>, Jian-Min Wang<sup>2</sup>

<sup>1</sup> *Department of Physics and Institute of Theoretical Physics, Nanjing Normal University, Nanjing 210097, China*

<sup>2</sup> *Key Laboratory for Particle Astrophysics, Institute of High Energy Physics, Chinese Academy of Sciences, Beijing 100039,*

15 October 2018

## ABSTRACT

Using the properties of SDSS DR7 QSOs catalog from Shen et al., the Baldwin effect, its slope evolution, the underlying drive for a large sample of 35019 QSOs with reliable spectral analysis are investigated. We find that the Baldwin effect exists in this large QSOs sample, which is almost the same in 11 different redshift bins, up to  $z \sim 5$ . The slope is -0.238 by the BCES (C IV EW depends on the continuum), -0.787 by the BCES bisector. For 11 redshift-bins, there is an increasing of the Baldwin effect slope from  $z \sim 1.5$  to  $z \sim 2.0$ . From  $z \sim 2.0$  to  $z \sim 5.0$ , the slope change is not clear considering their uncertainties or larger redshift bins. There is a strong correlation between the rest-frame C IV EW and C IV-based  $M_{\text{BH}}$  while the relation between the C IV EW and Mg II-based  $M_{\text{BH}}$  is very weak. With the correction of C IV-based  $M_{\text{BH}}$  from the C IV blueshift relative to Mg II, we suggest that this strong correlation is due to the bias of the C IV-based  $M_{\text{BH}}$ , with respect to that from the Mg II line. Considering the Mg II-based  $M_{\text{BH}}$ , a medium strong correlation is found between the C IV EW and the Eddington ratio, which implies that the Eddington ratio seems to be a better underlying physical parameter than the central black hole mass.

**Key words:** quasars:emission lines — galaxies:active — black hole physics

## 1 INTRODUCTION

Broad emission lines are a prominent property of QSOs. The discovery of an anti-correlation between the equivalent width (EW) of C IV  $\lambda 1549$  emission line and its nearby continuum luminosity in QSOs rest frame (the Baldwin effect), was first made by Baldwin (1977) (e.g. see a review by Shields 2006). Over the past 30 years, a significant amount of effort has been expended to confirm this effect in C IV including other prominent emission lines (e.g., Ly $\alpha$ , C III, Si IV, Mg II, [O III], Fe K $\alpha$ ), as well as exploring its origin and evolution (e.g. Dietrich et al. 2002; Zhou et al. 2005; Netzer et al. 2006; Kong et al. 2006; Xu et al. 2008; Wu et al., 2009; Richards et al. 2011).

Although it is believed that the Baldwin effect exists for many UV/optical emission lines, its origin is still a problem to debate. Several interpretations about its origin have been proposed (e.g. Netzer et al. 1992; Dietrich et al. 2002; Shang et al. 2003; Baskin & Laor, 2004; Xu et al. 2008; Wu et al., 2009). One promising interpretation is the softening of the spectral energy distribution (SED) for increasing luminosity, which lowers the ion populations having high ionization potentials (e.g., Netzer et al. 1992; Dietrich et al. 2002).

With the progress in the virial mass of a supermassive black hole (SMBH,  $M_{\text{BH}}$ ), it provides the possibility to explore the underlying physical parameters for the origin of C

IV Baldwin effect, such as the Eddington ratio (i.e. the ratio of the bolometric luminosity to the Eddington luminosity,  $L_{\text{Bol}}/L_{\text{Edd}}$ ), the  $M_{\text{BH}}$ , and the luminosity dependence of metallicity (e.g. Dietrich et al. 2002; Shang et al. 2003; Warner et al., 2004; Baskin & Laor, 2004, 2005; Xu et al. 2008). The single-epoch virial  $M_{\text{BH}}$  can be calculated from the broad line width (e.g., H $\beta$ , H $\alpha$ , Mg II, C IV) and empirical luminosity-size relation (e.g. Kaspi et al. 2000; Bian & Zhao 2004; Vestergaard & Peterson 2006; Shen et al. 2011). The  $L_{\text{Bol}}$  can be calculated from the monochromatic luminosity by the correction factor estimated from the composite SED (e.g., Richard et al., 2006; Shen et al. 2011).

For PG QSOs sample, Baskin & Laor (2004) found a strong correlation between the C IV EW and  $L_{\text{Bol}}/L_{\text{Edd}}$ , and suggested that the  $L_{\text{Bol}}/L_{\text{Edd}}$  is the primary physical parameters driving the Baldwin effect. However, Shang et al. (2003) used the method of Spectral Principal Component (SPC) to find there is no correlation between the Baldwin effect and the  $L_{\text{Bol}}/L_{\text{Edd}}$  or the  $M_{\text{BH}}$  as underlying physical parameters. Nikolajuk & Walter (2012) found that weak line QSOs didn't follow the relation between C IV EW and  $L_{\text{Bol}}/L_{\text{Edd}}$  by Baskin & Laor (2004). However, these weak-line QSOs have the same x-ray-optical spectral index ( $\alpha_{\text{ox}}$ ), with respect to other normal QSOs. It was suggested that

the weak-line QSOs are caused by the possible low covering factor (Nikolajuk & Walter 2012).

In the past, most of the work was made by using relatively small samples. The Sloan Digital Sky Survey (SDSS) provides possibility for us to investigate the Baldwin effect in a larger QSOs sample (e.g. Xu et al., 2008; Richard et al., 2011). With SDSS DR5, Xu et al. (2008) used the result from the pipeline of SDSS spectral fit, which measured the line feature by a single Gaussian fit for the continuum subtracted spectrum. Xu et al. (2008) found that, up to  $z \approx 5$ , the slope of the Baldwin effect seems to have no effect of cosmological evolution. They also found the C IV EW has a stronger correlation with C IV-based  $M_{\text{BH}}$  than the  $L_{\text{Bol}}/L_{\text{Edd}}$ , suggesting that the  $M_{\text{BH}}$  is probably the primary drive for the Baldwin effect.

Recently, Shen et al. (2011) made a careful spectral analysis and gave a compilation of properties for 105783 QSOs from SDSS DR7 QSOs catalog. Here we use their data to reinvestigate the Baldwin effect for the C IV line and its origin. Our adopted sample is briefly described in §2, the results and the analysis are given in §3, and the conclusions are presented in §4.

## 2 SAMPLE

SDSS DR7 covers an imaging area of about 11663 square degrees and a spectroscopic area of about 9380 square degrees (Abazajian et al. 2009). Schneider et al. (2010) presented a quasars catalog from SDSS DR7, consisting of 105783 QSOs with  $M_i < -22$ , increasing by 30% with respect to that in DR5. The wavelength coverage of SDSS spectrum is 3800Å to 9200Å. In order to investigate the C IV line, we select 51523 QSOs with  $z \geq 1.5$  in SDSS DR7 QSOs.

Shen et al. (2011) carefully considered the UV/optical Fe II contribution, host contribution in low- $z$  QSOs, and multiple-Gaussian fit for four lines of H $\alpha$ , H $\beta$ , Mg II, C IV for the single-epoch virial SMBH mass calculation. In their SDSS spectral analysis, they remove the effects of Galactic extinction in the SDSS spectra, and shift the spectra to rest frame. They compiled these continuum and line properties, as well as radio, infrared, X-ray properties (Schneider et al. 2010).

Because adopting the properties of the rest-frame C IV EW,  $M_{\text{BH}}$  and  $L_{\text{Bol}}/L_{\text{Edd}}$  in Shen et al. (2011), we briefly described their spectral analysis. For the weakness of Fe II and not high enough signal-to-noise (SN) of C IV line, Shen et al. (2011) only reported their C IV measurements without the Fe II template fits, and emphasized that their C IV EWs may be averagely overestimated by 0.05 dex. They fit for the C IV line over the [1500Å, 1600Å] wavelength range, with multiple Gaussians. They didn't subtract the C IV narrow component (e.g., Sulentic et al. 2007). Considering the possible narrow or broad absorption features of the C IV line in high- $z$  QSOs, they masked out  $3\sigma$  outliers below the 20 pixel boxcar-smoothed spectrum during the fits for the narrow absorption, and performed a second fit excluding pixels below  $3\sigma$  of the first model fit for the broad absorption. They gave the BAL (broad absorption line) flag for SDSS DR7 QSOs. QSOs flagged as BAL QSOs are not used in our investigation of the Baldwin effect.

For QSOs with  $1.5 \leq z \leq 2.25$ , they also fit the Mg

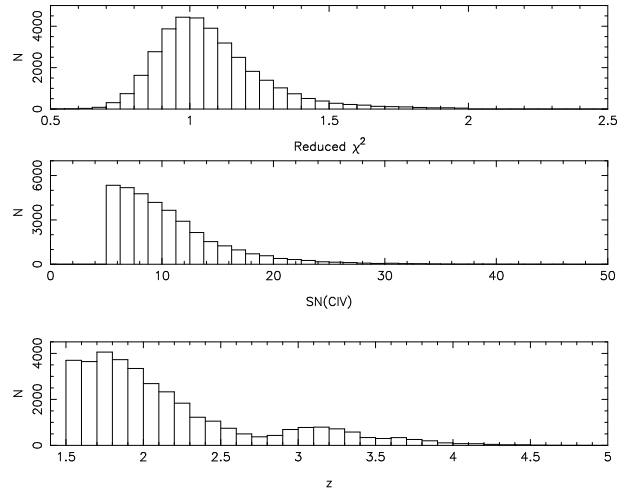


**Figure 1.** The distributions of the redshift  $z$ ,  $\text{SN}(\text{C IV})$ , and reduced  $\chi^2$ .

II emission line, as well as the SMBH mass from Mg II line. They fit for the Mg II line over the [2700Å, 2900Å] wavelength range, with a single Gaussian (with FWHM  $< 1200 \text{ km s}^{-1}$ ) for the narrow component, and for the broad component with a single Gaussian or multiple Gaussians. They provided a new mass calibration from Mg II lines by their multiple-Gaussian fits with narrow line subtraction, which is adopted as the fiducial virial SMBH mass for QSOs with  $0.9 \leq z < 1.9$ . For  $z \geq 1.9$ , they adopted the formulae of Vestergaard & Peterson (2006) to calculate the C IV virial mass.

We use following criteria to select our sample:  $z \geq 1.5$ ,  $\text{FWHM}(\text{C IV}) > 1200 \text{ km s}^{-1}$ , reduced  $\chi^2 < 2.0$ ,  $\text{EW}(\text{C IV}) > 2.0$ ,  $\text{SN}(\text{C IV}) > 5$ , excluding BAL QSOs. The number of our QSOs sample is 35019 ( $\sim 68\%$  of 51523 QSOs). Their distributions of the redshift, SN, and reduced  $\chi^2$  are showed in Figure 1. For the SMBH mass, we adopted their fiducial virial masses from Mg II for  $z < 1.9$  and masses from C IV for  $z > 1.9$ . The numbers are 14652, 19476, respectively (Shen et al. 2011). In Xu et al. (2008), there are 26623 QSOs used to investigate the C IV Baldwin effect, and 13960 QSOs used to investigate the relation of C IV EW with the accretion parameters ( $M_{\text{BH}}$ ,  $L_{\text{Bol}}/L_{\text{Edd}}$ ).

## 3 RESULTS AND DISCUSSION

### 3.1 The relation between the rest-frame C IV EW and $L_{1350}$

The following formula is used to express the relation between the C IV EW and the continuum luminosity at 1350 Å ( $L_{1350}$ ),

$$\log \text{EW}(\text{C IV}) = \alpha + \beta \log L_{1350} \quad (1)$$

Figure 2 gives the relation between the C IV EW and  $L_{1350}$  for 35019 QSOs from SDSS DR7. For the total 35019 QSOs, the spearman's rank correlation coefficient is  $R = -0.33$  and the null hypothesis is less than  $10^{-4}$ .

The regression analyzes are performed using the bivariate correlated errors and intrinsic scatter (BCES) algorithm

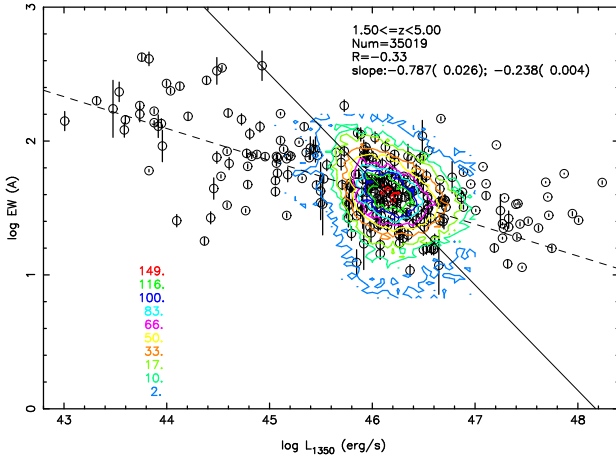


**Figure 2.** log-log correlation between the C IV EW and the continuum luminosity at 1350Å (in  $\text{erg s}^{-1}$ ) for the DR7 sample of 35019 QSOs with  $1.5 \leq z < 5.0$ . In the left bottom corner, the numbers for colorful contour levels are shown. The solid line is the linear fit from the BCES bisector and the bootstrap simulation. The dash line is BCES with EW(C IV) as the dependent variable and  $L_{1350}$  as the independent variable. In the right top corner, the redshift coverage, the number of the sample, the spearman's rank correlation coefficient, and the slopes with BCES( $Y|X$ ) and BCES bisector are listed. Black circles are data from a compiled sample of Wu et al. (2009).

(Akritas & Bershadsky 1996). There exists some difference between the BCES( $Y|X$ ) [i.e.,  $Y = f(X)$ ] and BCES( $X|Y$ ) [i.e.,  $X = g(Y)$ ] regressions. The bisector bisects these two regressions. The BCES regression is quite robust; bootstrapping simulations reproduce the theoretically expected results well (see, e.g., Akritas & Bershadsky 1996). For the SDSS sample, with the BCES( $Y|X$ ) ( $X$  is  $L_{1350}$ ), the slope is  $\beta = -0.238 \pm 0.040$ , and the intercept is  $\alpha = 12.6 \pm 0.19$ . However, with the BCES bisector, the slope is  $\beta = -0.787 \pm 0.026$ , and the intercept is  $\alpha = 37.9 \pm 1.20$  (see Table 1).

In Figure 2, we also plot their compiled sample from Wu et al. (2009). Their compiled sample consists of 272 AGNs: 189 from SDSS, 47 from HST, and 36 from IUE. They used two Gaussian profiles to fit the C IV emission lines after subtracting the power-law continuum. The continuum luminosity at the rest-frame 2500Å in Wu et al. (2009) is converted to the luminosity at the rest-frame 1350Å by assuming  $f_\nu \propto \nu^{-0.44}$  (i.e., larger by  $\sim 0.12\text{dex}$ , Vanden Berk et al. 2001). In Figure 2, the data of Wu et al. (2009) are consistent with our SDSS DR7 sample, as well as the dash line from BCES( $Y|X$ ). For their compiled sample of Wu et al. (2009), there are 163 common QSOs in our SDSS DR7 sample. For these 163 common QSOs, the C IV EWs from Wu et al. (2009) are consistent with that from Shen et al. (2009) very well, their C IV EW ratio has a normal distribution with mean 0.01 and dispersion 0.12.

For 81 PG QSOs from Baskin & Laor (2004), 454 Large Bright Quasar Survey objects by Forster et al. (2001) and 125 pre-COSTAR AGN by Kuraszkiewicz et al. (2002), we also find that these QSOs/AGNs are located in the region of SDSS QSOs or consistent with the dash line from BCES( $Y|X$ ) if they are scaled to our Figure 2.

The Baldwin effect provides a potential method to infer the luminosity of a QSO from its C IV observation. With

respect to classical standard candles of type Ia supernovae (SNe), QSOs can be observed to a much higher redshift. For our SDSS DR7 sample, we find the relation between  $L_{1350}$  and rest-frame C IV EW by BCES ( $Y|X$ ), BCES bisector, respectively:

$$\log L_{1350} = (-0.511 \pm 0.042) \log \text{EW(C IV)} + (46.977 \pm 0.066)$$

$$\log L_{1350} = (-1.271 \pm 0.043) \log \text{EW(C IV)} + (48.179 \pm 0.068)$$

From above formula, we can calculate the rms values of the residuals after subtracting the predicted luminosity from the measured C IV EW. We find that they are 0.286, 0.345, respectively. In order to use QSOs as standard candles via the Baldwin effect, it is suggested that we should at least confine the luminosity within an uncertainty of 30%,  $\sim 0.13$  dex (Wu et al., 2009). Therefore, it is impossible to use our QSOs data-set as standard candles via the Baldwin effect.

### 3.2 The slope of the Baldwin effect

In previous studies, the slope of the Baldwin effect is  $-0.14 \sim -0.20$  (see Table 1 in Xu et al. 2008 and reference therein). Dietrich et al. (2002) found the slope becomes steep for luminous QSOs, from  $-0.14$  for their total sample to  $-0.20$  for QSOs with  $\log \lambda L_\lambda(1450\text{\AA}) \geq 44 \text{ erg s}^{-1}$ . We get a slope from the BCES( $Y|X$ ),  $\beta = -0.238 \pm 0.04$  (Table 1), which is steeper than some previous studies. By BCES bisector, the slope is  $\beta = -0.787 \pm 0.026$ . The slope of BCES bisector ( $-0.787$ ) is more consistent with the slope of the "intrinsic" Baldwin effect, ( $\beta = -0.72$ ) by Pogge & Peterson (1992). Considering the compiled sample from Wu et al. (2009), the slope from the BCES( $Y|X$ ) is better than the slope of BCES bisector when wide luminosity range for QSOs are concerned (Figure 2).

The redshift coverage of our sample is from 1.5 to 5.0 (see Figure 1). In order to investigate the relation of the Baldwin effect with the redshift, We divide our sample into 11 bins according to the redshift, and the redshift bins are 1.5-1.6, 1.6-1.7, 1.7-1.8, 1.8-1.9, 1.9-2.0, 2.0-2.1, 2.1-2.25, 2.25-2.5, 2.5-3.0, 3.0-3.5, 3.5-5.0 (Table 1). The number in different redshift bins is about 3000. For different redshift bins, we calculate the spearman's rank correlation coefficient, the null possibility, the slopes and the intercepts with the BCES ( $Y|X$ ) and the BCES bisector (Table 1). Except the highest bin ( $3.5 \leq z < 5.0$ ), We find a medium strong correlation for different redshift bins ( $|R| \geq 0.3$ ).

It seems that there is an increase of the slope from  $z \sim 1.5$  to  $z \sim 2$  (Figure 3), which is the same to that by the BCES ( $Y|X$ ) and BCES bisector. From  $z \sim 2$  to  $z \sim 5$ , the slope evolution is not clear due to the large uncertainties. If we believe that the Baldwin effect is due to the softening of SED for increasing luminosity, the slope evolution from  $z \sim 1.5$  to  $z \sim 2$  implies the evolution of QSOs SED below  $z \sim 2$ . It is also possibly related to the covering factor evolution. In low redshift bins, the dynamical range in luminosity is larger due to the flux-limited nature of the sample, which might affect the linear regression. For redshift bins below  $z = 2.0$ , in the same luminosity range, i.e.,  $10^{45.6}$  to  $10^{46.6} \text{ erg s}^{-1}$ ,

**Table 1.** The C IV EW and the continuum luminosity Regression Parameters.  $\log \text{EW}(\text{C IV}) = \alpha + \beta \log L_{1350}$ .

$z$ (1)	N (2)	R (3)	$\beta^1$ (4)	$\alpha^1$ (5)	$\beta^2$ (6)	$\alpha^2$ (7)	$P_{\text{null}}$ (8)
SDSS DR7 sample							
1.5-5.0	35019	-0.33	$-0.238 \pm 0.040$	$12.6 \pm 0.19$	$-0.787 \pm 0.026$	$37.9 \pm 1.20$	$1.15 \times 10^{-25}$
SDSS DR7 sample in different $z$ bins							
1.5-1.6	3699	-0.33	$-0.386 \pm 0.021$	$19.4 \pm 0.98$	$-1.065 \pm 0.015$	$50.2 \pm 0.70$	$3.90 \times 10^{-4}$
1.6-1.7	3645	-0.32	$-0.292 \pm 0.016$	$15.0 \pm 0.75$	$-0.911 \pm 0.020$	$43.5 \pm 0.93$	$8.93 \times 10^{-4}$
1.7-1.8	3727	-0.35	$-0.283 \pm 0.013$	$14.6 \pm 0.58$	$-0.887 \pm 0.014$	$42.4 \pm 0.63$	$2.65 \times 10^{-5}$
1.8-1.9	4057	-0.35	$-0.272 \pm 0.012$	$14.1 \pm 0.57$	$-0.845 \pm 0.014$	$40.5 \pm 0.65$	$5.29 \times 10^{-5}$
1.9-2.0	3343	-0.31	$-0.233 \pm 0.013$	$12.3 \pm 0.60$	$-0.830 \pm 0.014$	$39.9 \pm 0.63$	$2.73 \times 10^{-3}$
2.0-2.1	2687	-0.32	$-0.230 \pm 0.015$	$12.2 \pm 0.70$	$-0.858 \pm 0.015$	$41.2 \pm 0.67$	$6.10 \times 10^{-3}$
2.1-2.25	3265	-0.33	$-0.249 \pm 0.013$	$13.1 \pm 0.62$	$-0.850 \pm 0.016$	$40.9 \pm 0.74$	$1.32 \times 10^{-3}$
2.25-2.5	3173	-0.34	$-0.273 \pm 0.014$	$14.2 \pm 0.64$	$-0.840 \pm 0.015$	$40.4 \pm 0.67$	$4.99 \times 10^{-4}$
2.5-3.0	2740	-0.34	$-0.279 \pm 0.015$	$14.5 \pm 0.69$	$-0.845 \pm 0.023$	$40.7 \pm 1.06$	$9.22 \times 10^{-4}$
3.0-3.5	3213	-0.30	$-0.238 \pm 0.014$	$12.6 \pm 0.66$	$-0.698 \pm 0.242$	$33.9 \pm 11.2$	$7.52 \times 10^{-3}$
3.5-5.0	1470	-0.27	$-0.215 \pm 0.022$	$11.5 \pm 1.04$	$-0.031 \pm 0.696$	$2.93 \pm 32.4$	$1.59 \times 10^{-1}$
SDSS DR7 sample in different $z$ bins ( $10^{45.6} \leq L_{1350} \leq 10^{46.6} \text{ erg s}^{-1}$ )							
1.5-1.6	3566	-0.30	$-0.387 \pm 0.023$	$19.4 \pm 1.05$	$-1.140 \pm 0.015$	$53.8 \pm 0.70$	$4.74 \times 10^{-3}$
1.6-1.7	3474	-0.28	$-0.293 \pm 0.018$	$14.9 \pm 0.83$	$-0.997 \pm 0.018$	$47.5 \pm 0.81$	$1.43 \times 10^{-2}$
1.7-1.8	3836	-0.31	$-0.287 \pm 0.016$	$14.7 \pm 0.74$	$-0.919 \pm 0.012$	$44.1 \pm 0.55$	$1.41 \times 10^{-3}$
1.8-1.9	3518	-0.31	$-0.280 \pm 0.016$	$14.5 \pm 0.73$	$-0.882 \pm 0.052$	$37.6 \pm 0.24$	$3.52 \times 10^{-3}$
1.9-2.0	3136	-0.27	$-0.230 \pm 0.016$	$12.2 \pm 0.75$	$-0.828 \pm 0.011$	$38.9 \pm 0.53$	$3.48 \times 10^{-2}$

<sup>1</sup>:BCES( $Y|X$ ) where  $Y$  is  $\text{EW}(\text{C IV})$  as the dependent variable, and  $X$  is  $L_{1350}$  as the independent variable. <sup>2</sup>:BCES bisector result.

we find  $R$  is  $\sim -0.3$ , and the slopes are consistent with the results for the total sample in different redshift bins (Table 1).

With SDSS DR5, Xu et al. (2008) used the SpecLine table to investigate C IV Baldwin effect. The SpecLine table is from the pipeline of SDSS spectral fit. The C IV line feature is measured by a single Gaussian fit for the continuum-subtracted spectrum. Xu et al. (2008) investigated the C IV Baldwin effect in the observed frame. In Xu et al. (2008), there was no correction of Galactic extinction for the  $L_{1350}$  and the C IV EW was given in the observed frame. In Figure 4, we showed a comparison of C IV EW in the rest frame for 10232 common QSOs from the current sample and Xu et al. (2008). We find that, the rest-frame C IV EW from the current sample is averagely larger by 0.23 dex than that from Xu et al. (2008). The difference is due to the spectral fitting, such as a single Gaussian fit for C IV in Xu et al. (2008), multiple-Gaussian fit in Shen et al. (2011).

### 3.3 The relation between C IV EW and $M_{\text{BH}}$ or $L_{\text{Bol}}/L_{\text{Edd}}$

The underlying physical origin for the Baldwin effect is still an open question. The fundamental process in QSOs is the accretion around the SMBHs. Using the data from Shen et al. (2011), we also investigate the relation between the rest-frame C IV EW and  $M_{\text{BH}}$  or  $L_{\text{Bol}}/L_{\text{Edd}}$  (Figure 5). For the total sample, we find a medium strong correlation between the rest-frame C IV EW and  $M_{\text{BH}}$  with  $R = -0.27$ , and the null hypothesis is less than  $10^{-4}$ . However, the correlation between the C IV EW and  $L_{\text{Bol}}/L_{\text{Edd}}$  is very weak,  $R = 0.01$  (Figure 5). Earlier studies on individual sources suggest that for the same object, an intrinsic Baldwin effect

does exist (albeit with a different slope), therefore, luminosity does drive the Baldwin effect (for the same object, it is equivalent to say that  $L_{\text{Bol}}/L_{\text{Edd}}$  drives the Baldwin effect). We find that the very weak correlation between C IV EW and  $L_{\text{Bol}}/L_{\text{Edd}}$  for the total SDSS DR7 sample is due to the mixed use of Mg II-based and C IV-based  $M_{\text{BH}}$  estimates.

For QSOs with  $z \geq 1.9$ , we use the mass from the C IV line, while the mass from Mg II line for QSOs with  $1.5 \leq z < 1.9$  (Shen et al. 2011). So, we divide the total our sample into two samples, i.e.,  $1.5 \leq z < 1.9$  and  $z \geq 1.9$ . For QSOs with  $1.5 \leq z < 1.9$ , We find a very weak correlation of  $R = 0.07$  between the rest-frame C IV EW and mass from the Mg II line. For the physical drive of the Baldwin effect,  $L_{1350}$  and  $M_{\text{BH}}$  are two essentially independent quantities. To understand which one is a better physical drive on the Baldwin effect, one needs to look at them separately, i.e., at fixed  $L_{1350}$  or fixed  $M_{\text{BH}}$ . Using the whole sample with mixed  $M_{\text{BH}}$  and  $L_{1350}$  makes it difficult to isolate the two. For  $L_{1350}$  between  $10^{45.7}$  and  $10^{46.5} \text{ erg s}^{-1}$ , we divide the total SDSS sample into four luminosity bins ( $\Delta \log L_{1350} = 0.2$ ), and find that this correlation between C IV EW and  $M_{\text{BH}}$  is stronger ( $R \sim 0.18$ ) than that for the total SDSS sample ( $R \sim 0.07$ ). For QSOs with  $z \geq 1.9$ , we find a strong correlation of  $R = -0.48$  between the C IV EW and C IV-based  $M_{\text{BH}}$  (Table 2; Figure 6). It is consistent with our previous result where we used the C IV FWHM from the standard pipeline of SDSS to calculate the single-epoch  $M_{\text{BH}}$  (Vestergaard & Peterson 2006; Xu et al. 2008). In section 3.4, the bias in C IV-based  $M_{\text{BH}}$  will be discussed.

For QSOs with  $1.5 \leq z < 1.9$ , we find a modest correlation between C IV EW and  $L_{\text{Bol}}/L_{\text{Edd}}$  ( $R = -0.28$ ). Because Mg II-based  $M_{\text{BH}}$  is proportional to  $v^2 \times R_{\text{BLR}}$ , and  $R_{\text{BLR}} \propto L_{1350}^{0.62}$  (Shen et al. 2011),  $L_{\text{Bol}}/L_{\text{Edd}}$  is proportional



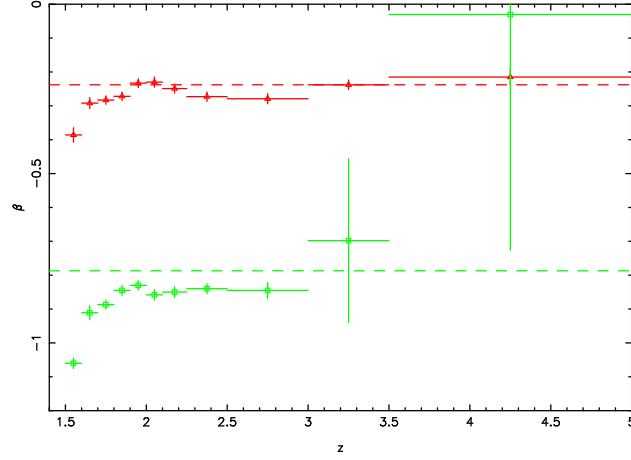


**Figure 3.** The slope versus the redshift. The red points are for the slopes by the BCES( $Y|X$ ). The green ones are for the slopes by the BCES bisector. The red/green dash lines are for the slopes for the total sample, respectively by the BCES( $Y|X$ ) and bisector.

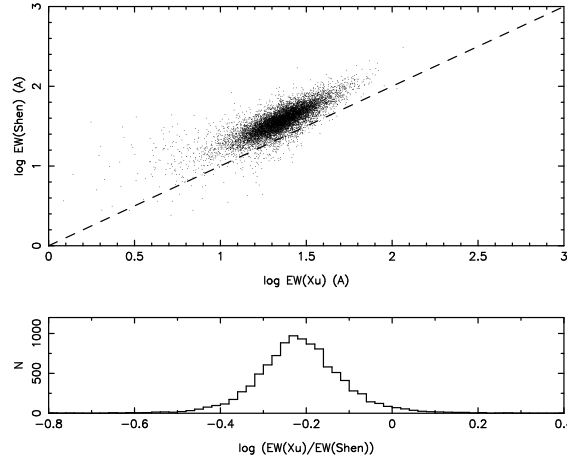


**Figure 4.** Top: A comparison of the rest-frame C IV EW for 10232 common QSOs from the current sample and Xu et al. (2008). The dash line is 1:1. Bottom: the distribution of the EW ratio of QSOs from Xu et al. (2008) to the current sample.

**Table 2.** The C IV EW drive Regression Parameters.  $\log \text{EW}(\text{C IV}) = \alpha + \beta \log L_{1350}$ ,  $\log \text{EW}(\text{C IV}) = \alpha + \beta \log M_{\text{BH}}$ , or  $\log \text{EW}(\text{C IV}) = \alpha + \beta \log L_{\text{Bol}}/L_{\text{Edd}}$ .

Drive (1)	$z$ (2)	N (3)	R (4)	$\beta^1$ (5)	$\alpha^1$ (6)	$\beta^2$ (7)	$\alpha^2$ (8)
$L_{1350}$	1.5-5.0	35019	-0.33	$-0.238 \pm 0.040$	$12.6 \pm 0.19$	$-0.787 \pm 0.026$	$37.9 \pm 1.20$
	1.5-1.9	15128	-0.34	$-0.299 \pm 0.076$	$15.4 \pm 0.35$	$-0.920 \pm 0.007$	$44.0 \pm 0.34$
	1.9-5.0	19891	-0.31	$-0.226 \pm 0.051$	$12.0 \pm 0.23$	$-0.755 \pm 0.057$	$36.5 \pm 2.63$
$M_{\text{BH}}$	1.5-5.0	34128	-0.27	$-0.125 \pm 0.011$	$2.74 \pm 0.10$	$-0.731 \pm 0.025$	$8.34 \pm 0.23$
	1.5-1.9	14652	0.07	$0.665 \pm 0.087$	$0.985 \pm 0.08$	$0.959 \pm 0.057$	$-7.22 \pm 0.05$
	1.9-5.0	19476	-0.48	$-0.178 \pm 0.019$	$32.3 \pm 0.18$	$-0.521 \pm 0.052$	$6.41 \pm 0.49$
$L_{\text{Bol}}/L_{\text{Edd}}$	1.5-5.0	34128	0.01	$0.272 \pm 0.001$	$1.58 \pm 0.01$	$0.182 \pm 0.091$	$1.77 \pm 0.83$
	1.5-1.9	14652	-0.28	$-0.268 \pm 0.080$	$1.41 \pm 0.06$	$-0.858 \pm 0.080$	$0.992 \pm 0.07$
	1.9-5.0	19476	0.26	$0.0003 \pm 0.00009$	$1.57 \pm 0.01$	$0.090 \pm 0.067$	$1.69 \pm 0.07$

<sup>1</sup>:BCES( $Y|X$ ) where Y is EW(C IV) as the dependent variable, and X is  $L_{1350}$ ,  $M_{\text{BH}}$ ,  $L_{\text{Bol}}/L_{\text{Edd}}$  as the independent variable, respectively. <sup>2</sup>:BCES bisector result.

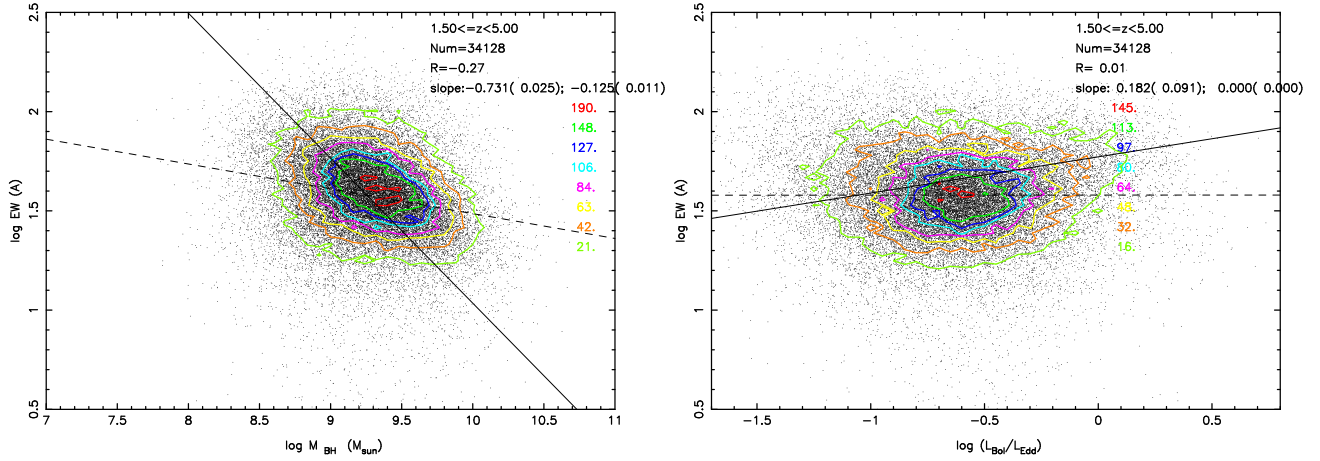


**Figure 5.** log-log correlation between the rest-frame C IV EW and the  $M_{\text{BH}}$  (left),  $L_{\text{Bol}}/L_{\text{Edd}}$  (right). In the right of two panels, the numbers for colourful contour levels are shown. The solid line is the linear fit from the BCES bisector and the bootstrap simulation. The dash line is BCES with EW(C IV) as the dependent variable and  $M_{\text{BH}}/L_{\text{Bol}}/L_{\text{Edd}}$  as the independent variable. In the right top corner, the redshift coverage, the number of the sample, the spearman's rank correlation coefficient, the slopes and their errors with BCES( $Y|X$ ) and BCES bisector are listed.

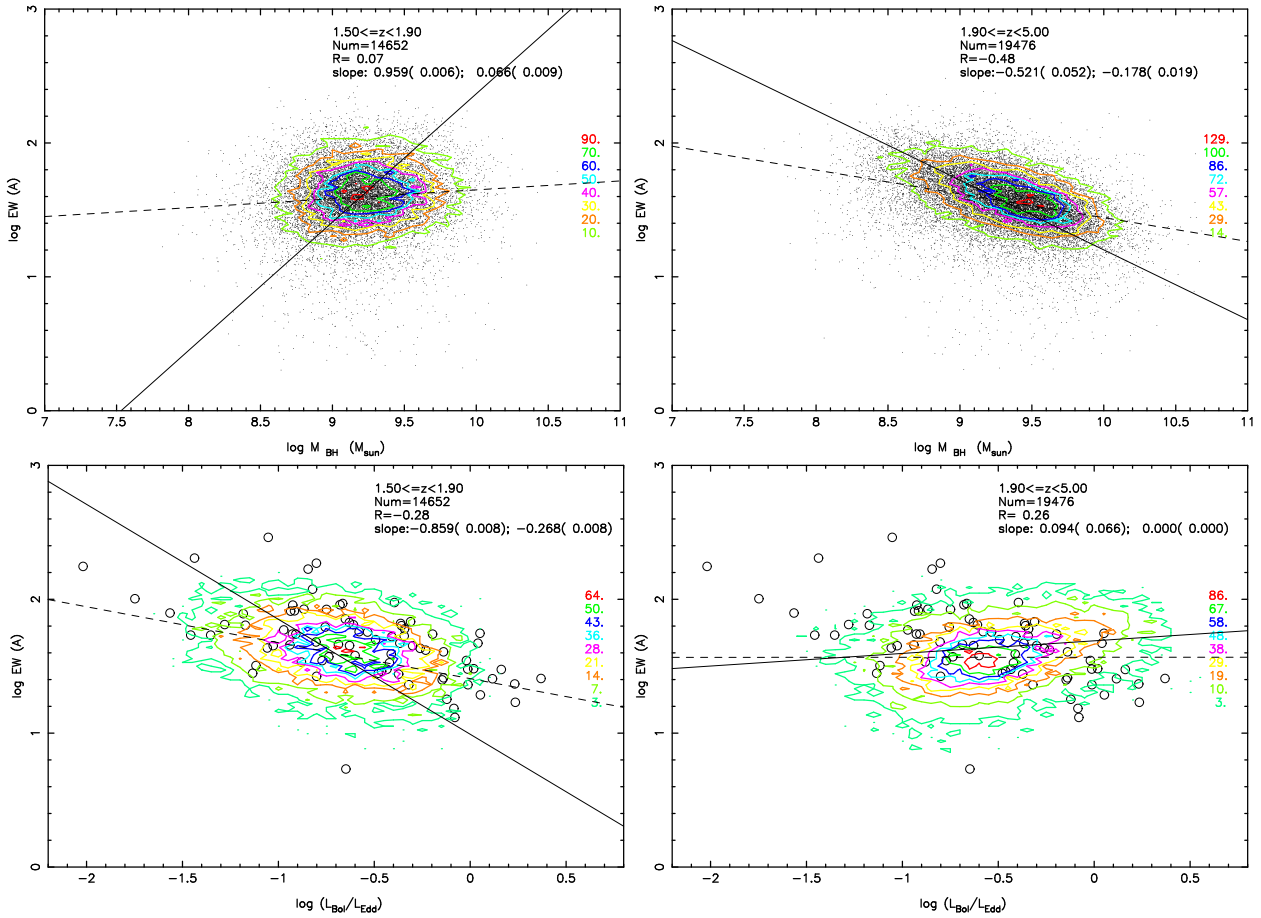


**Figure 6.** log-log correlation between the rest-frame C IV EW and the  $M_{\text{BH}}$  (top),  $L_{\text{Bol}}/L_{\text{Edd}}$  (bottom) for two redshift bins,  $1.50 \leq z < 1.9$ ,  $z \geq 1.9$ . In the right of four panels, the numbers for colourful contour levels are shown. The solid line is the linear fit from the BCES bisector and the bootstrap simulation. The dash line is BCES with EW(C IV) as the dependent variable and  $M_{\text{BH}}/L_{\text{Bol}}/L_{\text{Edd}}$  as the independent variable. In the right top corner of four panels, the redshift coverage, the number of the sample, the spearman's rank correlation coefficient, the slopes and their errors with BCES( $Y|X$ ) and BCES bisector are listed. Black circles in two bottom panels are data from Baskin & Laor (2004).

to  $L_{1350}^{0.38}$  neglecting the effect of Mg II FWHM. We find that  $\text{EW}(\text{CIV}) \propto (L_{\text{Bol}}/L_{\text{Edd}})^{-0.27}$  for QSOs with  $1.5 \leq z < 1.9$  by BCES( $Y|X$ ). Using this correlation, we can derive the expected Baldwin effect of  $\text{EW}(\text{CIV}) \propto L_{1350}^{-0.10}$ , however, the slope of Baldwin effect (Table 1) is -0.24. It suggests that the relation between C IV EW and  $L_{\text{Bol}}/L_{\text{Edd}}$  is not completely from the relation between C IV EW and  $L_{1350}$ . We use partial Kendalls  $\tau$  to investigate the role of  $L_{1350}$  in the relation between C IV EW and  $L_{\text{Bol}}/L_{\text{Edd}}$  for the total sample. We find that the relation between C IV EW and  $L_{\text{Bol}}/L_{\text{Edd}}$  is weakened when  $L_{1350}$  is held fixed. The partial Kendalls  $\tau$  is -0.135 for QSOs with  $1.5 \leq z < 1.9$ , and 0.097 for QSOs with  $1.9 \leq z < 5.0$ , while their spearman's rank correlation coefficients are -0.28 and 0.26 (Table 2). It is possible that  $L_{\text{Bol}}/L_{\text{Edd}}$  is not very important in controlling the Baldwin effect, or that the large uncertainty of individual  $M_{\text{BH}}$  estimates is diluting any inherent correlation.

In Figure 6, we also show the location of low- $z$  PG QSOs from Baskin & Laor (2004), where the  $M_{\text{BH}}$  was calculated from the  $\text{H}\beta$  FWHM. These PG QSOs, which are denoted by black circles in Figure 6, are consistent well with our sample of  $1.5 \leq z < 1.9$  QSOs where Mg II-based  $M_{\text{BH}}$  is used. However, these PG QSOs don't follow the relation found for  $1.9 \leq z < 5.0$  QSOs where C IV-based  $M_{\text{BH}}$  is used. With respect to  $\text{H}\beta$ -based  $L_{\text{Bol}}/L_{\text{Edd}}$ , it was found that the relation between  $\text{EW}(\text{C IV})$  and  $L_{\text{Bol}}/L_{\text{Edd}}$  is weaker when  $L_{\text{Bol}}/L_{\text{Edd}}$  is based on the C IV FWHM (Baskin & Laor 2005). Considering the strong correlation between C IV EW and  $L_{\text{Bol}}/L_{\text{Edd}}$  for low- $z$  PG QSOs found by Baskin & Laor (2004), our result also shows a strong bias of C IV-based  $M_{\text{BH}}$ , with respect to Mg II-based  $M_{\text{BH}}$ .

### 3.4 The C IV-based $M_{\text{BH}}$ correction from the C IV blueshift relative to Mg II

However, we should keep in mind that the underlying physical drive analysis depends on the  $M_{\text{BH}}$  calculation. The bias of  $M_{\text{BH}}$  calculated from Mg II, C IV are investigated (e.g., Rafiee & Hall 2011; Shen et al. 2012). It is found that the C IV-based  $M_{\text{BH}}$  is biased to the possible non-virialized component in C IV (Shen et al., 2008; Richard et al. 2011; Shen et al. 2011; Shen et al. 2012). The Mg II-based  $M_{\text{BH}}$  can be calibrated to yield consistent virial mass estimates with those based on the  $\text{H}\alpha$ / $\text{H}\beta$ , while the C IV-based  $M_{\text{BH}}$  is poorly correlated with the  $\text{H}\beta$ -based  $M_{\text{BH}}$  or  $\text{H}\alpha$ -based  $M_{\text{BH}}$  (Shen et al. 2012). It was found that the C IV blueshift relative to  $\text{H}\beta$  can be used as a C IV FWHM correction (shen et al. 2012). For 24228 QSOs with  $1.5 \leq z \leq 2.25$ , we find a strong correlation between C IV-based  $M_{\text{BH}}$  and the C IV blueshift relative to Mg II ( $\Delta V = v_{\text{off,CIV}} - v_{\text{off,MgII}}$ ),  $R = -0.41$ . We also find a strong correlation between C IV EW and the C IV blueshift relative to Mg II,  $R = -0.38$  (bottom left panel in Figure 7;  $R = -0.11$  when only using the C IV blueshift). This strong correlation between C IV EW and the C IV blueshift relative to Mg II is consistent with the disk+wind model (Richards et al. 2011). It is possible that QSOs with larger C IV blueshift have softer SEDs and have a larger radiation line driving contribution to their winds to dominate over the disk.

The C IV blueshift relative to Mg II would lead to the apparent correlation between C IV EW and C IV-based  $M_{\text{BH}}$ . We can use the C IV blueshift relative to Mg II to do the

C IV-based  $M_{\text{BH}}$  correction. Shen et al. (2011) gave the Mg II-based  $M_{\text{BH}}$  and C IV-based  $M_{\text{BH}}$  for QSOs with  $1.5 \leq z \leq 2.25$  (their Table 1). Their spearman's rank correlation coefficient is  $R = 0.28$  and the null hypothesis is less than  $10^{-4}$  (top left panel in Figure 7). We use the C IV blueshift relative to Mg II to do the correction of C IV-based  $M_{\text{BH}}$ . Using BCES regression analyzes, we find a strong correlation between the  $M_{\text{BH}}$  difference ( $\log M_{\text{BH,MgII}} - \log M_{\text{BH,MgII}}$ ) and the C IV blueshift relative to Mg II,  $R = -0.44$  (top right panel in Figure 7):

$$\log M_{\text{BH,MgII}} - \log M_{\text{BH,CIV}} = a + b(v_{\text{off,CIV}} - v_{\text{off,MgII}}) \quad (2)$$

Where  $a = (0.174 \pm 0.004)$ ,  $b = (-2.01 \pm 0.04) \times 10^{-4}$  by BCES( $Y|X$ ), and  $a = (0.449 \pm 0.007)$ ,  $b = (-5.78 \pm 0.08) \times 10^{-4}$  by BCES bisector.

Considering the correction of C IV-based  $M_{\text{BH}}$  from above formula, the spearman's rank correlation coefficient for the relation of Mg II-based  $M_{\text{BH}}$  and the corrected C IV-based  $M_{\text{BH}}$  changes from 0.28 to 0.38, 0.36, respectively. Using above formula by BCES( $Y|X$ ) and BCES bisector to do the C IV-based  $M_{\text{BH}}$  correction, we find that, for the relation between C IV EW and  $L_{\text{Bol}}/L_{\text{Edd}}$  for 9019 QSOs with  $1.9 \leq z \leq 2.25$ ,  $R$  changes from 0.22 to -0.03, -0.29, respectively (bottom right panel). And for the relation between C IV EW and the corrected C IV-based  $M_{\text{BH}}$ ,  $R$  changes from -0.45 to -0.24, 0.1, respectively. They are consistent with the results for 14652 QSOs with  $1.5 \leq z \leq 1.9$  where Mg II-based  $M_{\text{BH}}$  is used.

### 3.5 The origin of the Baldwin effect

Considering Mg II-based  $M_{\text{BH}}$  (QSOs with  $z < 1.9$  QSOs), we find that the correlation coefficient for the relation between C IV EW and  $L_{1350}$  ( $R = -0.34$ ) is larger than the other two relations (i.e. C IV EW versus  $M_{\text{BH}}$ , C IV EW versus  $L_{\text{Bol}}/L_{\text{Edd}}$ ;  $R = 0.07, -0.28$ ). And the correlation coefficient of C IV EW with  $L_{\text{Bol}}/L_{\text{Edd}}$  ( $R = -0.28$ ) is larger than that of C IV EW with  $M_{\text{BH}}$  ( $R = 0.07$ ). It is consistent with the result by Baskin & Laor (2004). The stronger correlation between C IV EW and  $M_{\text{BH}}$  in Xu et al. (2008) is due to the usage of C IV-based  $M_{\text{BH}}$ . Therefore, by the larger sample, we find that C IV EW is primarily controlled by the  $L_{1350}$ , with respect to  $L_{\text{Bol}}/L_{\text{Edd}}$  and  $M_{\text{BH}}$ . The modest correlation between C IV EW and the  $L_{\text{Bol}}/L_{\text{Edd}}$  (larger than that between C IV EW and  $M_{\text{BH}}$ ) implied that the  $L_{\text{Bol}}/L_{\text{Edd}}$  seems to be a better underlying physical parameter than  $M_{\text{BH}}$ . The strong correlation between the C IV EW and C IV blueshift relative to Mg II is in favor of the disk+wind model (e.g. Richards et al. 2011). The QSOs with larger C IV blueshift have softer SEDs and have a larger radiation line driving contribution to their winds to dominate over the disk.

## 4 CONCLUSIONS

With respect to our previous analysis for SDSS DR5 QSOs, we use the SDSS DR7 QSOs catalog from Shen et al. (2011) to reinvestigate the Baldwin effect, its slope evolution, the underlying drive. The main conclusions can be summarized as follows: (1) The Baldwin effect exists in the large sample

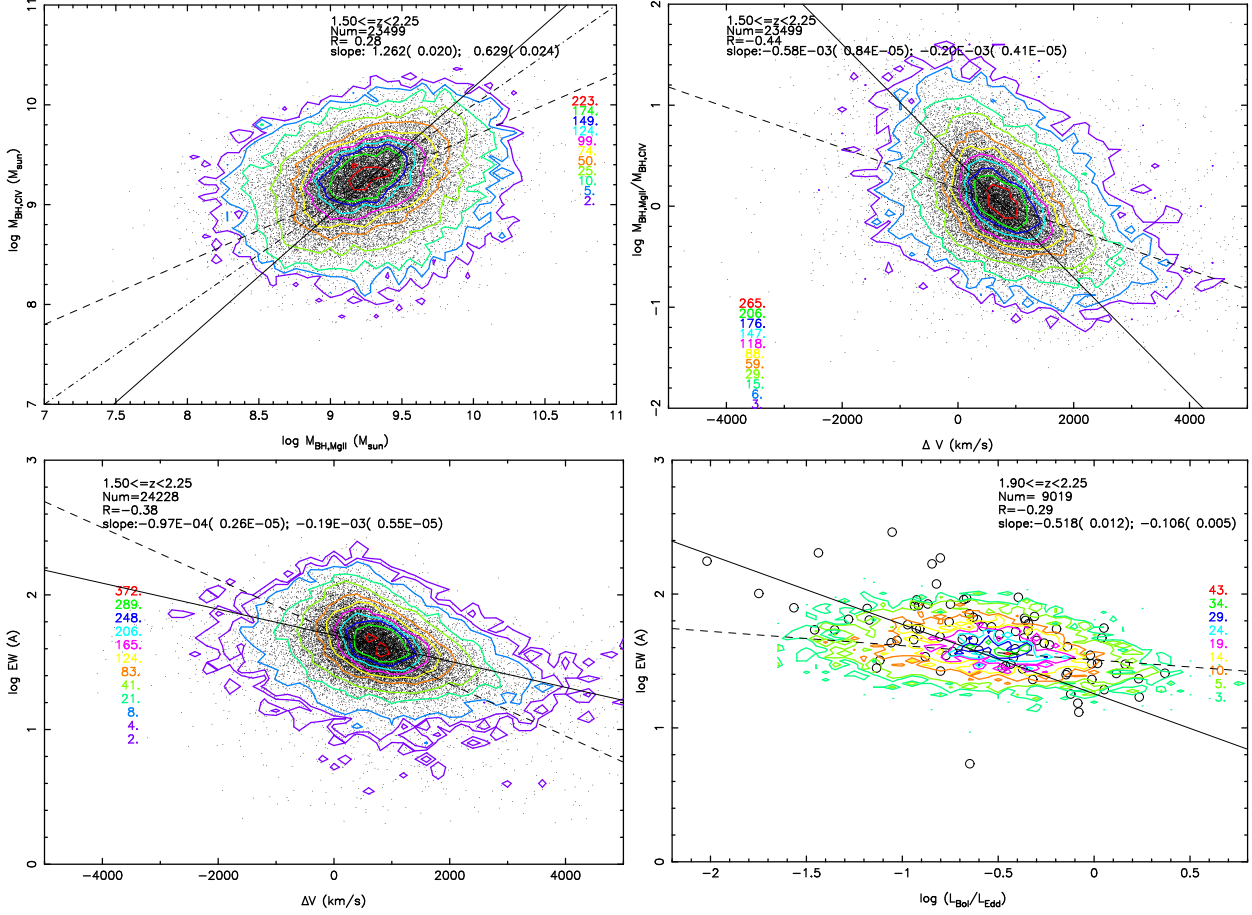


**Figure 7.** Top left: C IV-based  $M_{\text{BH}}$  versus Mg II-based  $M_{\text{BH}}$ . Top right: The ratio of Mg II-based  $M_{\text{BH}}$  to C IV-based  $M_{\text{BH}}$  versus the C IV blueshift relative to Mg II. Bottom left: C IV EW versus the C IV blueshift relative to Mg II. Bottom right: C IV EW versus the corrected C IV-based  $L_{\text{Bol}}/L_{\text{Edd}}$  (for clarity, the data points are not shown). The numbers for colorful contour levels are shown in different panels. The solid line is the linear fit from the BCES bisector and the bootstrap simulation. The dash line is BCES with Y as the dependent variable and X as the independent variable. In the top corner of four panels, the redshift coverage, the number of the sample, the spearman's rank correlation coefficient, the slopes and their errors with BCES(Y|X) and BCES bisector are listed. Black circles in the bottom right panel are data from Baskin & Laor (2004).

of 35019 QSOs with reliable spectral analysis. The correlation coefficient is  $R = -0.33$ , which is almost the same for QSOs in different redshifts, up to  $z \sim 5$ . (2) For the total sample, the slope is  $-0.238$  by the BCES (C IV EW depends on  $L_{1350}$ ),  $-0.787$  by the BCES bisector. (3) For 11 redshift bins, there is an increasing of the Baldwin effect slope from  $z \sim 1.5$  to  $z \sim 2.0$ . From  $z \sim 2.0$  to  $z \sim 5.0$ , the slope change is not clear considering their uncertainties or the larger redshift bin. (4) By 34128 QSOs with  $M_{\text{BH}}$  and  $L_{\text{Bol}}/L_{\text{Edd}}$  carefully derived from spectral decomposition by Shen et al. (2011), we find that there is a strong correlation between the rest-frame C IV EW and C IV-based  $M_{\text{BH}}$  for  $1.9 \leq z < 5.0$  ( $R = -0.48$ ). However, the relation between C IV EW and Mg II-based  $M_{\text{BH}}$  for  $1.5 \leq z < 1.9$  is very weak ( $R = 0.07$ ). We think it is due to the bias of the C IV-based  $M_{\text{BH}}$ , with respect to the Mg II-based  $M_{\text{BH}}$ . Using the correction of C IV-based  $M_{\text{BH}}$  from the C IV blueshift relative to Mg II, we find the correlation of C IV EW with corrected C IV-based  $M_{\text{BH}}$  becomes weak (from  $R = -0.45$  to  $R = 0.1$ ). Considering the Mg II-based  $M_{\text{BH}}$ , a medium strong correlation is found between C IV EW and  $L_{\text{Bol}}/L_{\text{Edd}}$

( $R = -0.28$ ), which implies that the  $L_{\text{Bol}}/L_{\text{Edd}}$  seems to be a better underlying physical parameter than  $M_{\text{BH}}$ .

## 5 ACKNOWLEDGMENTS

We thank the discussion during the LAMOST science meeting at April, 2012. We thank an anonymous referee for suggestions that led to improvements in this paper. This work has been supported by the National Science Foundations of China (No. 11173016; 11233003).

## REFERENCES

- Akritis M. G. & Bershadsky M. A., 1996, ApJ, 470, 706
- Abazajian K. N., et al. 2009, ApJS, 182, 543
- Baskin A., Laor A., 2004, MNRAS, 350, L31
- Baskin A., Laor A., 2005, MNRAS, 356, 1029
- Baldwin J.A., 1977, ApJ, 214, 679
- Bian W., Zhao Y. 2004, MNRAS, 347, 607
- Dietrich M., Hamann F., Shields J.C. et al., 2002, ApJ, 581, 912
- Forster K., et al., 2001, ApJS, 134, 35



- Kong M. Z. et al., 2006, *A&A*, 456, 473
- Kaspi, S., Smith, P.S., Netzer, H., Maoz, D., Jannuzi, B.T., Giveon, U. 2000, *ApJ*, 533, 631
- Kuraszkiewicz J. K., et al., 2002, *ApJS*, 143, 257
- Netzer H., Laor A., & Gondhalekar P. M. 1992, *MNRAS*, 254, 15
- Netzer H., Mainieri V., Rosati P., Trakhtenbrot B., 2006, *A&A*, 453, 525
- Nikolajuk M., Walter R., 2012, *MNRAS*, 420, 2518
- Pogge R. W., & Peterson B. M., 1992, *AJ*, 103, 1084
- Rafiee A., Hall P. B. 2011, *MNRAS*, 415, 2932
- Richards G. T., et al. 2006, *ApJS*, 166, 470
- Richards G. T., et al. 2011, *AJ*, 141, 167
- Schneider D. P., et al. 2010, *AJ*, 139, 2360
- Shields J. C., in *Proceedings of The Central Engine of Active Galactic Nuclei*, ed. L. C Ho & J.-M. Wang (San Francisco: ASP), p.355
- Shang Z., et al., 2003, *ApJ*, 586, 52
- Shen Y., et al., 2008, *ApJ*, 680, 169
- Shen Y., et al., 2011, *ApJS*, 194, 45
- Shen Y., & Liu X., 2012, *ApJ*, 753, 125
- Sulentic J. W., Bachev R., Marziani P., Negrete C. A., Dultzin D., 2007, *ApJ*, 666, 757
- Vanden Berk, et al., 2001, *AJ*, 122, 549
- Vestergaard M., Peterson B. M., 2006, *ApJ*, 641, 689
- Warner C., Hamann F., Dietrich M., 2004, *ApJ*, 608, 136
- Wu J., et al., 2009, *ApJ*, 702, 767
- Xu Y., Bian W. H., Yuan Q. R., Huang K., L., 2008, *MNRAS*, 389, 1703
- Zhou X.-L., & Wang J.-M. 2005, *ApJ*, 618, L83